

## IMPACT OF FORCED AERATION ON VERTICAL FLOW TREATMENT WETLAND PERFORMANCES FOR COMBINED SEWER OVERFLOW

Daniella Portela<sup>a,\*</sup>, Katharina Tondera<sup>b</sup>, Stéphane Troesch<sup>c</sup>, Pascal Molle<sup>a</sup>

<sup>a</sup> INRAE, REVERSAAL, F-69625 Villeurbanne, France

<sup>b</sup> Université Claude Bernard Lyon 1, LEHNA UMR 5023, CNRS, ENTPE, F-69518 Vaulx-en-Velin, France

<sup>c</sup> Ecobird, 69630 Chaponost, France

### ARTICLE INFO

#### Keywords:

Forced aeration strategy  
Hydraulic loads  
Nitrification  
Bioretention filters  
CSO-TW

### ABSTRACT

Combined Sewer Overflow Treatment Wetlands (CSO wetlands) are designed to remove pollutants under stochastic events with variable hydraulic loads. Upgrading them with forced aeration promises to increase the effectiveness and resilience of the treatment. We have tested two vertical CSO wetlands with forced aeration (CSOa and CSOb) to understand the effects of aeration on CSO treatment. Both filter beds have 0.95 and 0.80 m of saturated layer. CSOa uses gravel as top filtering layer, while CSOb utilizes sand and an additional transition layer. Tracer tests were conducted in both filters with and without aeration to assess the impact of aeration on hydraulic performance. CSOa operated with four different aeration conditions, with the optimal condition tested on both filters for comparison. Samples were taken for analysis of global parameters and the redox potential was monitored online. In the tracer test, CSOa allowed to observe the mixing impact of aeration, which avoids any preferential path when influent entered the filter. The addition of a sand layer at the surface (CSOb) allows for a more even distribution of water on the top, which limits preferential flows when aeration is off. In both filters, the results showed that aeration increased the residence time and mixing degree ( $NTIS < 3$ ). Testing different aeration strategies revealed the dependence of dissolved pollutant removal on oxygen supply. In CSOa, the median outlet concentration varied from 23 to 6.4  $\text{mg.L}^{-1}$  in TSS, 153 to 32  $\text{mg.L}^{-1}$  total COD (CODt), 124 to 20  $\text{mg.L}^{-1}$  soluble COD (CODs) and 5 to 2.5  $\text{mg.L}^{-1}$   $\text{NH}_4\text{-N}$  according to aeration strategy. The lower outlet concentrations were always under the highest aeration condition. Under the optimal condition (75 min on/15 min off), median removal of CSOa was 97% TSS, 85% CODt, 78% CODs and 75%  $\text{NH}_4\text{-N}$ . Besides COD and TSS, outlet concentration and removal efficiency did not significantly differ between CSOa and CSOb. Pollutant removal demonstrated a linear correlation with organic surface load. Overall, forced aeration in CSO-TW distinctly affected filter dynamics and improved its performance.

### 1. Introduction

As rainfalls have a stochastic feature, infrastructure managing stormwater needs to be adapted to receive inflows with a high level of variability in terms of volume, pollutant loads, frequency and intensity (Gioia et al., 2021; Seidl et al., 1998). Unlike steady inflow in domestic wastewater treatment systems, facilities treating overflows from combined sewers operate under specific conditions that influence effluent concentrations (Kadlec and Wallace, 2008). The proportions of stormwater (SW) and domestic wastewater (WW) in combined sewer systems (CSS) are between 4:1 to 100:1 during rain events (Tondera et al., 2021). Madoux-Humery et al. (2015) and Phillips et al. (2012) observed a large

number of contaminants in the frequently occurring combined sewer overflows (CSOs), resulting from the re-suspension of sewer deposits and suspended solids from runoff. Episodes of heavy rain events are likely to intensify due to global warming (IPCC, 2023), increasing concerns of greater spill frequency, volume and impact of CSO pollution on receiving waters. Urban expansion, marked by increased construction and reduced infiltration areas, further increase SW flow in combined sewer systems (Salerno et al., 2018). Implementing facilities to treat CSO emerges as a viable technical solution to protect surface water and water pollution control (Oral et al., 2020).

French regulation requires that CSO treatment wetlands, regardless of discharge location, guarantee at least the same outlet concentrations

\* Corresponding author.

E-mail address: [daniella.goncalves-portela@inrae.fr](mailto:daniella.goncalves-portela@inrae.fr) (D. Portela).

<https://doi.org/10.1016/j.ecoleng.2024.107359>

Received 15 January 2024; Received in revised form 5 July 2024; Accepted 31 July 2024

Available online 14 August 2024

0925-8574/© 2024 The Authors. Published by Elsevier B.V. This is an open access article under the CC BY-NC-ND license (<http://creativecommons.org/licenses/by-nc-nd/4.0/>).

as required at wastewater treatment plants of the same catchment area. This necessitates the use of a treatment technology that is able to maintain performance when operating under extremely varying conditions. Treatment wetlands (TWs) intended for CSO treatment are Nature Based Solutions (NBSs) adaptable to the local context. They work by retaining water to attenuate peak flows and removing pollutants (Dou et al., 2017; Stefanakis, 2019). Different variations of CSO wetlands have been implemented according to national regulation approaches (Germany, France, and Italy (Dotro et al., 2017; Rizzo et al., 2020)). Nevertheless, it is essential to undertake a meticulous design process and, in certain instances, to implement optimization measures in order to comply with the most rigorous regulatory standards.

In classical vertical CSO wetlands, the top layer has a depth of  $>0.45$  m and up to 1 m, followed by a drainage layer, which can be saturated or not, and it can have a transient layer between the two layers. The indicated media for the filtration layer is sand (0–2 mm) with at least  $10^{-4}$  m/s of hydraulic conductivity (Dotro et al., 2017). In Germany, there is a recommendation to add 20% of limestone to the filtration substrate to keep the pH buffering capacity (DWA-A178, 2019). The drainage layer at the bottom is 0.20–0.30 m in depth and consists of 16–22 mm coarse gravel. Some vertical CSO wetlands maintain a saturated zone to prevent the loss of plants during dry weather periods, dilute high inflow concentrations and avoid hydraulic short cuts (Pálffy et al., 2017c).

Pollutant removal in vertical CSO wetlands mainly occurs in the upper layer through filtration, adsorption and biological degradation. An aerobic environment favors organic matter removal and nitrogen oxidation (Ruppelt et al., 2018; Uhl and Dittmer, 2005). Design guidelines for vertical CSO wetlands (e.g. ANR, 2013; DWA-A178, 2019) include a throttle to control the outflow and a freeboard for water retention, ensuring hydraulic peak attenuation and that a minimum hydraulic retention time is maintained during peak hydraulic loading events.

Every vertical CSO wetland system has a pollutant removal capacity that depends on internal or external factors. For example, filter design and operation favor certain groups of bacteria (aerobic/anaerobic). Presence, abundance and therefore performance of these bacteria depend on factors such as hydraulic and organic loads, as well as influent quality. In the CSO wetland, COD removal rates of approx. 80% and total suspended solids (TSS) removal of 50 to 90% have been observed (Ruppelt et al., 2019; Tondera et al., 2013). Masi et al. (2017) observed a mass reduction of 93% of the ammonium-nitrogen ( $\text{NH}_4\text{-N}$ ) inflow load. Additionally, for events occurring in summer, the outlet concentration was close to zero at the end of an event. To be efficient and consistent in particulate organic matter removal and nitrification, CSO wetland design has to be robust and perform effectively across in a wide range of rainfall events (Pálffy et al., 2017b).

Despite vertical CSO wetlands' efficient removal capacity of organic matter, there is a need to enhance the removal of dissolved pollutants and to create conditions to promote effective denitrification (Rizzo et al., 2020). It is essential to ensure aerobic conditions when the surface of the filter is covered with water since anaerobic conditions can inhibit or slow down the degradation of major pollutants such as COD and  $\text{NH}_4\text{-N}$  (Uhl and Dittmer, 2005). Furthermore, traditional vertical CSO wetlands undergo a two-step process of ammonia transformation. First, adsorption occurs during feeding phases, when the filter is submerged. Then, in between events during dry weather, nitrification occurs in the unsaturated filtration layer converting  $\text{NH}_4\text{-N}$  to nitrogen-nitrate ( $\text{NO}_3\text{-N}$ ). Denitrification is unlikely to occur in this second step due to the aerobic predominance. During the subsequent event,  $\text{NO}_3\text{-N}$  is flushed out in significant quantities at the outset (Pálffy et al., 2017c). Consequently, total nitrogen outlet concentrations are highly fluctuating. Additionally, long-lasting events or those with high concentrations of dissolved COD can push the system functioning to a limit since biological degradation processes depend on oxygen conditions and hydraulic residence time (HRT) (Rizzo et al., 2020).

The incorporation of forced aeration into TWs for the treatment of domestic and industrial wastewaters has demonstrated promising results in achieving enhanced treated effluent quality beyond that achieved in classical TWs (Boog et al., 2014; Murphy et al., 2016; Nivala et al., 2019). Enhancing internal mixing, optimizing hydraulic retention time, and controlling oxygen conditions improve both pollutant removal and system resilience (Boog et al., 2018; Headley et al., 2013; Miyazaki et al., 2023). However, to our best knowledge, studies on TWs with forced aeration treating CSO have not been published.

In this context, this study aims to investigate the impact of aeration on the removal efficiency of specific dissolved pollutants and the system's resilience under high hydraulic loads. The research includes (i) analysis of system hydrodynamics in event-driven vertical flow wetlands under forced aeration, (ii) determining optimal aeration condition to nitrify ammonium-nitrogen and remove dissolved organic matter, and (iii) assessing aeration effects in different hydraulic loads.

## 2. Material and methods

### 2.1. Experimental systems

On the REFLET INRAE research Platform, France, Craponne,  $45^{\circ}44'11.5''\text{N}$   $4^{\circ}43'06.0''\text{E}$ , two aerated vertical CSO wetlands pilots (CSOa and CSOb) are installed, each having a surface area of  $20\text{ m}^2$ . The pilots were planted with 2.5 stems per  $\text{m}^2$  of common reed (*Phragmites australis*) in the middle of September 2022. Influent ( $12\text{ m}^3\cdot\text{h}^{-1}$ ) is distributed by a single feeding point in the middle from a suspended pipe that was positioned one meter above the surface. An outlet adjustable standpipe controls the saturated layer height, and a throttle controls the outflow rate. At the bottom of the filter are drainage pipes (diam. 125 mm) and aeration driplines of 16 mm internal diameter connected to an air blower (1.1 kW) that promotes forced aeration. Airflow, pressure and temperature can be measured by a vortex flowmeter EH Prowirl F200, a pressure transmitter BDSensors 18.601G for low pressure, and a platinum resistance thermometer EH iTHERM CompactLine.

The pilots operate in saturated conditions in the coarse gravel layer, with varying levels of saturation between pilots (Fig. 1). From bottom to top, the media within CSOa consists of a 0.95 m of coarse gravel (10/20 mm) covered with a layer of 0.20 m of gravel (2/4 mm), and those of within CSOb consists of 0.80 m of coarse gravel (10/20 mm) and is followed by a transient layer of 0.15 m of gravel (2/4 mm) and a filtering layer of 0.20 m of sand (0/4 mm). The permanent saturation level is of 0.95 m and 0.80 m for CSOa and CSOb, respectively.

### 2.2. Pilots' operation

The pilots were fed with pre-conditioned combined sewage (CS) to simulate CSOs. The CSO pilot feed is reproduced using real domestic WW from a combined sewer (city of Craponne) mixed with real storm water from a separate SW sewer that was stored in a  $200\text{ m}^3$  retention basin. Fresh domestic WW and stored SW were mixed during feeding in a unitary pipe in a way that typical ranges of physicochemical CSO characteristics were reached (Andrés-Doménech et al., 2018; Cross et al., 2021; Gasperi et al., 2012; Masi et al., 2017). This was done by mixing 1 part of wastewater with 4 to 11 parts of stormwater. To simulate the impact of different rainfall events, hydraulic loads (HL) of 0.5, 1.0 and  $1.5\text{ m}^3\cdot\text{m}^{-2}$  per event were selected. Once the feeding process was complete, drainage commenced until the permanent saturated water level was reached, which was controlled by the standpipe. Dry periods from 2 to 18 days were established in between each loading event.

Outflow throttling was adjusted to reach  $0.04\text{ L}\cdot\text{s}^{-1}\cdot\text{m}^{-2}$  at the highest water level (1.1 m on the filter surface). During an inflow event, the average airflow rate was maintained at  $1.15\text{ m}^3\cdot\text{m}^{-2}\cdot\text{h}^{-1}$ .

The oxygen consumption (OC) needed for pollutant degradation and mass oxygen transfer (OT), in each event were estimated using the eqs. 1

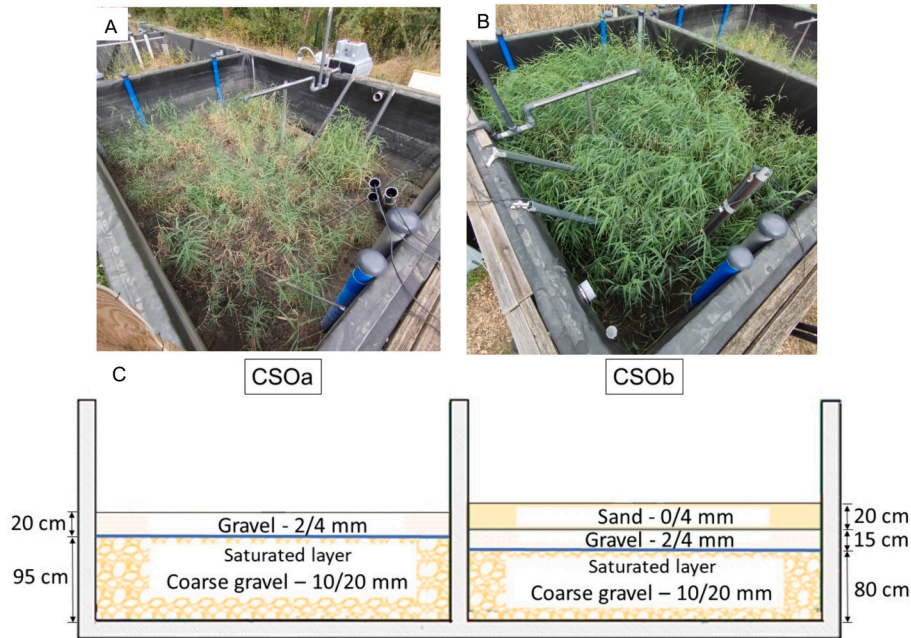


Fig. 1. Photo on the top left (A): top view of CSOa; top right (B): top view of CSOb. Vertical profile of CSOa and CSOb on the bottom (C).

and 2:

$$OC = Q * (\Delta COD + 4.5 * \Delta TKN) \quad (1)$$

$$OT = t_{aeration} * Q_{air} * \rho_{air} * m_{O_2/air} * SOTE \quad (2)$$

where:  $Q$  is the inflow ( $L \cdot d^{-1}$ );  $\Delta COD$  is the chemical oxygen demand consumed ( $mg \cdot L^{-1}$  – non biodegradable COD is neglected);  $\Delta TKN$  is the Total Kjeldahl Nitrogen consumed ( $mg \cdot L^{-1}$ );  $t$  is aeration time (h);  $Q_{air}$  is the delivered air flow from the blower ( $m^3 \cdot h^{-1}$ );  $\rho_{air}$  is the air density ( $kg \cdot m^{-3}$ ),  $m_{O_2/air}$  is the mass of oxygen in the air equal to 21% (in number of mols) and a Standard Oxygen Transfer Efficiency (SOTE) of 0.09. The SOTE was obtained from water column aeration tests (1 m in height) filled with gravel 10/20 mm (Séranne et al., 2021).

Different aeration strategies were applied in four phases on CSOa, increasing progressively the aeration time:

- 1) F10: air blower switched on for 10 min when feeding started then remained switched off during the rest of the event, including the drainage phase;
- 2) F10/40: only during the feeding phase, the air blower followed a cycle of 10 min on and 40 min off, and the drainage phase was carried out without aeration;
- 3) 10/40: during the feeding and drainage phase, the air blower followed a cycle of 10 min on and 40 min off;
- 4) 75/15: during the feeding and drainage phase, the air blower followed a cycle of 75 min on and 15 min off.

The simulated rainfall events on CSOb worked only under the aeration condition 75/15. Feeding (1 to 3 h), drainage (10 to 23 h) and air blowers' operation time (0.3 to 12.7 h) varied according to the hydraulic load. Consequently, higher hydraulic loads had longer total aeration time. During dry periods, the air blower was turned on for 10 min every 10 h to facilitate oxygen transfer in the deeper zones of the saturated layer.

### 2.3. Hydraulic characterization

To understand the hydrodynamics of the filter during the pollutant removal process, we conducted two tracer test campaigns, one with and

one without aeration. Combining two different tracers in one campaign allowed the evaluation of hydraulics (residence time, degree of mixing and presence of preferential path) before the ponding phase (at the beginning of an event) and once surface ponding (0.2 m) is present. This allows the impact of the ponding zone on tracer distribution at the surface, to be identified. Each campaign consisted of a pulse injection of fluorescein solution ( $0.14 \text{ g} \cdot L^{-1}$  and  $0.5 \text{ g} \cdot L^{-1}$  in CSOa and CSOb, respectively) into the inlet point when feeding started, then an Amino G acid solution ( $1.26 \text{ g} \cdot L^{-1}$  and  $1.5 \text{ g} \cdot L^{-1}$ , respectively) at the same point were injected when the ponding occurred. The tracer solutions were prepared with products from Thermo Scientific Chemicals. The outflow rate increased continuously until the second tracer was injected, and then the flow rate was maintained with the throttle at a consistent flow at the inlet and outlet.

A fluorimeter (TRMC-Fluo of Tetradre) was positioned at the outlet of each pilot to measure tracer fluorescence in mV, and the values were converted to  $mg \cdot L^{-1}$  with the help of calibration curves created in advance with the outlet water (data not shown).

The main hydraulic indicators, mean retention time ( $t_{mean}$ ) and number of tanks in series (TIS–N), were estimated using Eqs. 4 and 5. Residence Time Distribution  $E(t)$  (Eq. 3) is the normalization of output concentration measurement on time, wherein  $Q$  in  $m^3/h$  is the outflow and  $C$  in  $g/m^3$  is the outlet concentration of the tracer

$$E(t) = \frac{Q(t) * C(t)}{\int_0^{\infty} Q(t) * C(t) dt} \quad (3)$$

The gamma distribution determined N through error minimization of resultant  $E(t)$ , which was calculated with measured data. In this study, the used gamma distribution function is:

$$E(t)_{gamma} = \frac{N}{t_{mean} * \Gamma(N)} \left( \frac{N * t}{t_{mean}} \right)^{N-1} \exp \left( - \frac{N * t}{t_{mean}} \right) \quad (4)$$

wherein N is the number of complete stirred tanks in series;  $t$  (h) is time;  $t_{mean}$  (h) is the experimental HRT, and  $\Gamma(N)$  (h-1) is the gamma distribution, calculated with the SOLVER tool in Excel™. The experimental HRT  $t_{mean}$  is the integral over time and  $E(t)$  (Tchobanoglous et al., 2003):

$$t_{mean} = \int_0^{\infty} t * E(t) dt \quad (5)$$

The theoretical hydraulic residence time ( $t_t$ ) represents the ideal duration for the fluid spend in the filter and, ideally, it is equal to  $t_{\text{mean}}$ . However, dead zones or preferential paths reduces the time of the fluid in the filter, therefore, deviating  $t_{\text{mean}}$  from  $t_t$ . Plug flows and completely mixed tanks are ideal models, which do not occur undisturbed in practice. The calculated TIS-N is a hydraulic indicator showing if the hydraulics in the tested TW are closer to a plug flow ( $N = \infty$ ) or to a continuous stirred tank reactor (CSRT,  $N = 1$ ) reactor.

#### 2.4. Sampling procedure, water quality physicochemical and statistical analysis

After finishing the tracer tests on the pilot, continuous monitoring began with online sensors and sampling campaigns for laboratory analyses. The monitoring campaign lasted from March to October 2023 in CSOa and July to October 2023 in CSOb. Composite samples were taken by a programmed autosampler (ISCO 5800) throughout the feeding and drainage phases at the inlet and outlet of each pilot. At the inlet, 150 mL was sampled every 2 min (constant inflow), while at the outlet, 100 mL was sampled for every 200 L of effluent that passed through and discharged from each pilot. The samples were analyzed for the global parameters COD<sub>t</sub>, COD<sub>s</sub>, total suspended solids (TSS), ammonium-nitrogen (NH<sub>4</sub><sup>+</sup>-N), nitrite-nitrogen (NO<sub>2</sub><sup>-</sup>-N), and nitrate-nitrogen (NO<sub>3</sub><sup>-</sup>-N). With the total and soluble COD, particulate COD (COD<sub>p</sub>) was calculated. The laboratory analyses were conducted in accordance with the standards NF EN 872 and NF T 90-101 for TSS and COD as well as NF EN ISO 14911 and EN ISO 10304-1 for the ionic chromatography of NH<sub>4</sub><sup>+</sup>, NO<sub>2</sub><sup>-</sup>, NO<sub>3</sub><sup>-</sup>. Analyses of TKN (standard EN 25663) were also conducted to identify any non-dissolved forms of nitrogen and to allow calculation of total nitrogen removal and OC. Additionally, probes were placed inside the pilots at 60 cm from the bottom and at the outlet to monitor redox potential. This was found to be an indicator of biochemical reactions and microbial activity in CSO wetland pilots (Ruppelt et al., 2019).

Statistical analysis was done using MS Excel 2016 to obtain at the inlet and outlet minimum, maximum and median concentrations. The dataset distribution and the assessment of its normality was checked with plots in RStudio. In parallel, Fisher's F-test was performed to assess variance between the filters' dataset. If observed that data did not meet normal distribution or equal variance, the Mann-Whitney U test was used to compare CSOa and CSOb. Fisher's F-test and Mann-Whitney U test were calculated with RStudio for differences with a significance level of  $p < 0.05$ .

### 3. Results and discussion

#### 3.1. Tracer test

Each campaign lasted approx. 40 h, and the recovered mass of the tracer was between 77% and 97% (Table 1). Headley and Kadlec (2007) suggest that to validate a tracer test a minimum of 80% of the injected mass needs to be recovered at the outlet, hence, the results were

**Table 1**

Percentage of tracer mass recover, hydraulic indicators of theoretical and measured mean time.  $t_{10}$  and  $t_{90}$  are the time until 10% and 90% of the tracer mass leaves the filter, respectively, N, is the number of tanks in series.

	Without aeration				With aeration			
	Beginning		Ponding		Beginning		Ponding	
	CSOa	CSOb	CSOa	CSOb	CSOa	CSOb	CSOa	CSOb
Mass recover (%)	77	97.5	78	87.1	87	92.5	83	80.9
$t_t$ (h)	5	7	8	13.8	5	9	8	13.5
$t_{\text{mean}}$ (h)	2.3	5.6	7.6	9.1	8.1	10.9	6.5	10.5
$t_{10}$ (h)	0.5	2.1	3.9	5.3	2.3	3.7	1.6	3.9
$t_{90}$ (h)	4.7	9.9	12.1	13.3	15.5	19.8	12.9	18.9
NTIS	1.7	3	5.3	8	2.2	2.7	1.8	2.7

considered representatives for evaluating the TWs' hydrodynamics.

The theoretical residence time in the saturated zone was estimated by dividing the water volume in the saturated layer per mean outflow rate in the steady state. The transient flow rate until the establishment of ponding was not considered in this study to simplify HRT calculation. Fig. 2A shows the curve of outflow tracer mass over time for the tested conditions on CSOa.

At the start of feeding, an early peak with  $t_{\text{mean}} = 2.5$  h, appeared when aeration was off (Fig. 2A). While using aeration, the residence time in the saturated zone is longer. Once ponding occurs, inlet water is better distributed at the filter's surface, and the HRT of the two tested conditions was closer to  $t_t = 9.1$  h. Therefore, aeration appears to better mix the tracer in the whole volume and avoid short-circuiting at the beginning of an event.

Fig. 2B shows the bell shape in the dimensionless curves of residence time distribution (RTD). The RTD curve, representing the conditions without aeration, has different shapes from the beginning of the event to ponding. Ponding allows a better water distribution on the top and decreases preferential flows. In contrast, the event with aeration showed characteristics close to Continuous Stirred Tank Reactors (CSTR) from the beginning to the ponding.

In the CSOb filter, the lower permeability of the sand at the surface allows a better surface distribution of water at the beginning of an event. Consequently, preferential pathways were considerably reduced compared to CSOa. Fig. 2C shows the results of the outflow mass over time at the beginning and at the ponding phase of CSOb. The  $t_{\text{mean}}$  at the beginning of feeding was 5.6 h and in contrary to CSOa, there was no early peak. The  $t_{\text{mean}}$  of the ponding phase in CSOb without and with aeration were 9.1 h and 10.5 h, respectively, meaning that during the ponding the mean and theoretical HRT were almost equivalent regardless of aeration. Improvements due to forced aeration on CSOb were observed in the degree of mixing (Fig. 2D), which was similar to observations from CSOa. In the campaign with aeration, the RTD curves overlapped, indicating uniform mixing of the liquids in the filter.

The  $t_{\text{mean}}$ ,  $t_{10}$ , and  $t_{90}$ , were obtained using gamma distribution and are presented in Table 1, as well as the number of tanks in series and tracer mass recovery. The presence of tracer indicated by  $t_{10} = 0.5$  h in the test without aeration of CSOa leads to the conclusion that water percolates only in a small part of the saturated zone before leaving. Consequently, without aeration a large part of the filter (49%) acts as a dead zone in the beginning phase. Fournel (2012) and Pálffy et al. (2017c) observed preferential paths studying non-aerated vertical CSO wetlands; they explained the presence of short-circuiting when feeding starts with infiltration mainly limited to the area around the feeding point. Eventually, extended periods of low inflow may compromise the CSO wetlands treatment, although it remains negligible in events where ponding is rapidly established. In our study, we assume that air bubbles ascending through the filter media force tangential movements of particles moving downwards from the moment feeding starts, which increases the retention time and creates a stronger mixing pattern. Studies on wastewater treatment with TW have confirmed that dead zones and/or short-circuiting, which compromise the effluent treatment, can be

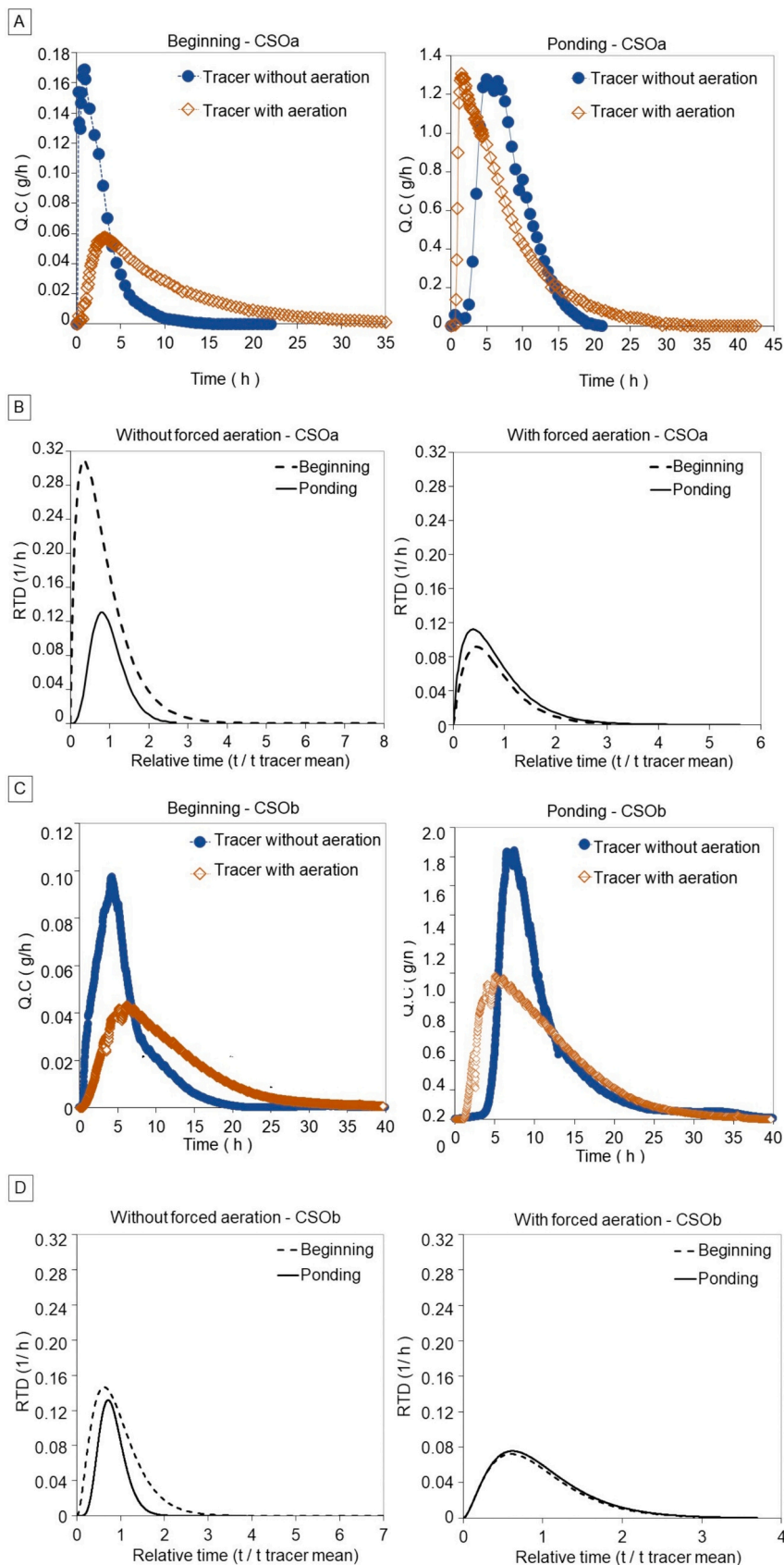


**Fig. 2.** A: Graphs of output mass curve in time for CSOa. B: Graphs of residence time distribution (RTD) in CSOa using Gamma distribution to fit experimental data. C: Graphs of output mass curve in time for CSOb. D: Graphs of residence time distribution (RTD) in CSOb using Gamma distribution to fit experimental data.

attenuated with forced aeration (Boog et al., 2014; Dotro et al., 2017).

Table 1 presents the impact of aeration on NTIS. The presence of aeration in both filters leads to NTIS around 2 for the saturated and ponding phases due to the improved of mixing degree. In a study by Boog et al. (2014) with an aerated vertical flow wetland treating domestic sewage, the authors observed similar hydraulic characteristics of the liquid within the filter since NTIS was close to 1 due to forced aeration. On the one hand, switching off aeration in the filter without sand results in a small NTIS of 1.7 at the beginning, but a significant dead zone and reduced HRT due to sub-optimal mixing. On the other hand, despite aeration, the presence of sand improves surface distribution and reduces the dead zone, but during the ponding phase, NTIS increases, indicating a flow pattern closer to a plug flow reactor.

### 3.2. Removal performances

#### 3.2.1. TSS and COD removal

Fig. 3 presents the inlet and outlet concentrations of the different aeration strategies for TSS and COD as measured in CSOa. Inlet concentrations were obtained by mixing WW and SW using ratios of 1:4 to 1:11 (as described in Section 2.2). Filtration is very efficient independently of aeration strategies. Outlet concentrations were always lower than 30 mg.L<sup>-1</sup> for TSS and in most cases, except during the F10 aeration strategy, they were below 12 mg.L<sup>-1</sup> (Table 2). The TSS concentrations at the outlet of CSOa and CSOb (Fig. 3 and Table 2) were comparable to conventional vertical CSO wetlands (Tondera, 2019) and TWs receiving SW with TSS concentrations similar to the ones in CSO (Schmitt et al., 2015).

For COD, the condition F10 in CSOa did not adequately degrade the CODs, leading to high outlet COD concentrations. During the F10 condition, the oxygen transferred to the water only meets 1 to 5% of the average oxygen demand of the influent, adversely affecting COD degradation. However, in other phases, COD degradation appears more efficient, consistently maintaining CODt outlet concentrations below 50 mg.L<sup>-1</sup> regardless of the aeration strategy. Oxygen transferred to the water ranged from 6 to 9%, 20–44%, and 50–100% of the average oxygen demand for the F10/40, 10/40, and 75/15 aeration strategies, respectively. The increase of oxygen diffusion in the filter creates zones for the growth of aerobic heterotroph bacteria (Vymazal, 1999). Due to the increased aeration times, certain aeration strategies resulted in lower COD<sub>t</sub> concentrations at the outlet, as shown in the results of Fig. 3 and Table 2. By changing the aeration strategy to the interval F10/40, the outlet stayed around 30 mg.L<sup>-1</sup> instead of 250 mg.L<sup>-1</sup> observed in the F10 aeration strategy. The performance was comparable to, or even better than in other studied CSO wetlands without primary settlement

Table 2

TSS, COD<sub>t</sub> and COD<sub>s</sub> values of minimum, maximum and median concentration at the inlet and outlet of CSOa and CSOb.

		Inlet concentration (mg. L <sup>-1</sup> )			Outlet concentration (mg. L <sup>-1</sup> )		
		TSS	COD <sub>t</sub>	COD <sub>s</sub>	TSS	COD <sub>t</sub>	COD <sub>s</sub>
CSOa	MIN	94	253	110	15	72	58
F10	MAX	485	455	315	30	252	226
(n = 7)	MEDIAN	159	348	183	23	153	124
CSOa	MIN	121	111	20	8	24	20
F10/40	MAX	149	179	62	12	38	28
(n = 3)	MEDIAN	133	119	34	12	37	24
CSOa	MIN	170	171	26	9	28	17
10/40	MAX	237	251	42	12	35	31
(n = 4)	MEDIAN	200	225	34	12	32	20
CSOa	MIN	120	116	55	6	23	10
75/15a	MAX	312	416	155	16	49	37
(n = 17*)	MEDIAN	155	223	112	6	32	25
CSOb	MIN	52	93	56	1	10	10
75/15b	MAX	315	308	200	11	35	30
(n = 19)	MEDIAN	133	207	90	4	27	18

\* For TSS n = 15.

that showed COD concentrations around 40 mg.L<sup>-1</sup> in the outlet (Masi et al., 2023; Pály et al., 2017a). Despite variations on hydraulic and pollutant loads, the outlet concentrations remained stable. It shows the resiliency of the aerated system, maintaining high retention of solids and COD degradation, in accordance with other CSO wetland systems (Rizzo et al., 2020).

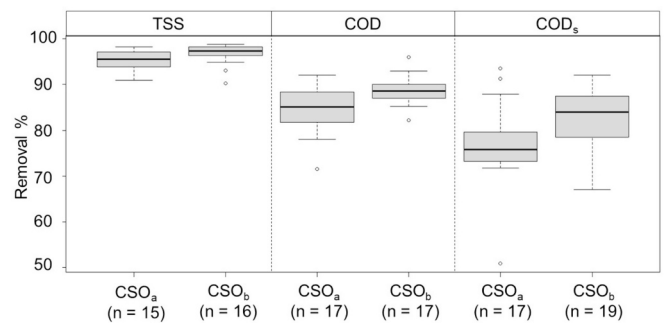


Fig. 4. Tukey's boxplot of removal performance of TSS, COD and dissolved COD in the filters CSOa (n = 17 for COD and COD<sub>s</sub> and n = 15 for TSS) and CSOb (n = 19) under the aeration condition 75/15.

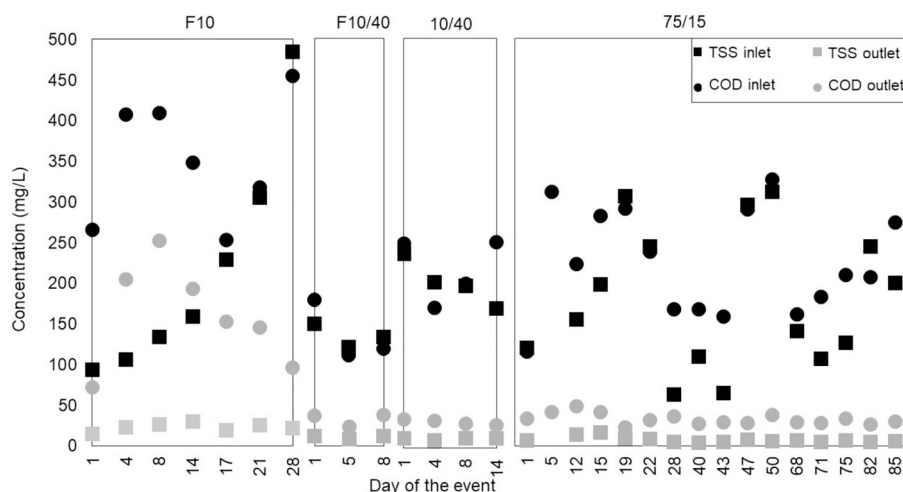


Fig. 3. Inlet and outlet concentrations of TSS and COD under each tested aeration condition in CSOa (F10, F10/40, 10/40 and 75/15).

The median outlet concentrations and removal efficiencies resultant from tests in CSOa and CSOb are presented in Table 2 and Fig. 4.

When comparing CSOa and COSb under condition 75/15, the addition of a sand layer resulted in an improvement of TSS removal ( $p = 0.045$ ). However, both filters consistently demonstrated TSS removal rates of  $>90\%$  (Fig. 4). There was a significant difference in the removal of CODt between CSOa and CSOb ( $p = 0.002$ ), as well as a significant difference in the CODt outlet concentrations between the filters ( $p = 0.008$ ). The CODs removal efficiency did not show significant differences between the performances of the two filters ( $p = 0.162$ ). The median concentrations of effluent CODt were  $32 \text{ mg.L}^{-1}$  in CSOa and  $27 \text{ mg.L}^{-1}$  in CSOb, which is in accordance with studies of Pálffy et al. (2017b) and Dittmer (2006). In some events, the effluent concentration was  $10 \text{ mg.L}^{-1}$ . These results are below the concentrations observed in the studies of Pálffy et al. (2017a) and Dittmer (2006). It is likely that the higher CODt removal on CSOb is due to the lower concentration of TSS at the CSOb outlet ( $p = 0.009$ ), as the sand layer can retain more solids. The 83% median removal of TSS in CSOa is not far from 89% removal in CSOb but CSOb had less variation than CSOa.

Independently of inlet variations, the removal efficiencies of CODt and CODs for both CSOa and CSOb were high. For example, removal efficiency of both filters under the 75/15 aeration strategy, showed a COD removal of consistently above 70% in all events (Fig. 4).

In the above-mentioned studies on none-aerated vertical CSO wetlands by Dittmer (2006) and Pálffy et al. (2017a),  $<50\%$  of CODs removal were found. Depending on the system design, the treatment process has low CODs removal due to the absence of aeration during feeding (saturated conditions) (Meyer et al., 2013). Generally, the adsorption characteristics of the filter material together with the characteristics of localized bacterial communities in the filter play an important role in CODs removal (Pálffy et al., 2017a). A dry period of longer than 10 days leads to the susceptibility of microorganism dehydration. When the next event begins, the transfer of electrons in water and adsorption processes are hindered as microorganisms strive to reach their saturation levels, thereby limiting the degradation of dissolved pollutants (Uhl and Dittmer, 2005). The studied systems minimized the dehydration issue with a permanently saturated layer of almost 1 m depth. While studies using passive aeration have generally shown low removal efficiency of CODs, under the specific condition created by aeration strategy of 75/15, the median CODs removal efficiency reached 75% in CSOa and 82% in CSOb. This shows that forced aeration in CSO wetlands can maintain high oxidizing conditions and thus degrade dissolved organic compounds.

### 3.2.2. Removal of nitrogen forms

The resulting inlet and outlet concentrations of nitrogen forms from 31 events loaded into CSOa (Fig. 5) showed  $\text{NO}_2\text{-N}$  concentration remaining below  $1.60 \text{ mg.L}^{-1}$  in all conditions, irrespective of the aeration strategy. As expected the concentrations of  $\text{NO}_2\text{-N}$  are low due to its unstable oxidative form in TWs (Kadlec and Wallace, 2008). However, the effects of aeration on  $\text{NH}_4\text{-N}$  and  $\text{NO}_3\text{-N}$  forms were noticeable. The median  $\text{NH}_4\text{-N}$  outlet concentrations from all strategies tested on CSOa ranged from 3 to  $6 \text{ mg.L}^{-1}$ . However, the 75/15 aeration strategy demonstrated the lowest variation in  $\text{NH}_4\text{-N}$  outlet concentrations, even at the highest inlet concentrations (Fig. 6).

The calculation of oxygen transfer considered the oxygen consumed in the process of organic matter degradation and nitrogen transformation. The lack of oxygen in the condition F10 compromised both organic matter and  $\text{NH}_4\text{-N}$  removal. However, covering at least 20% of the oxygen demand in the condition created by the 10/40 aeration strategy tests improved  $\text{NH}_4\text{-N}$  removal. For a larger range of inlet concentration, the 75/15 aeration strategy demonstrated greater resilience to outlet variation of  $\text{NH}_4\text{-N}$ , even when the oxygen transferred was lower than the oxygen demand (calculated by Eqs. 1 and 2). Although these calculations are approximate, they nevertheless enable us to estimate the aeration times required to maintain efficient nitrification.

Under the 75/15 aeration strategy and until day 43,  $\text{NH}_4\text{-N}$  was  $<6 \text{ mg.L}^{-1}$  at the outlet when inlet concentrations were  $< 20 \text{ mg.N.L}^{-1}$ . In addition, on days 1, 40, 68, 71 and 82 of the 75/15 aeration operation, the sum of inorganic nitrogen concentrations at the outlet showed 5 to  $2 \text{ mg.N.L}^{-1}$  more than the concentrations measured at the inlet. Besides possible analytical uncertainties, mineralized compounds from plants and microorganisms lead to the release of nitrogen and an imbalance of inorganic nitrogen concentration at the inlet and outlet, as observed in the study of Collins et al. (2010). Thus, this factor can cause an elevation of inorganic nitrogen in the outlet compared to concentrations measured at the inlet.

In filters with passive aeration, dry periods shorter than 5 days have a negative impact on  $\text{NH}_4\text{-N}$  removal by reducing the filter's adsorption capacity (Dittmer, 2006; Uhl and Dittmer, 2005). Seasonality is another factor influencing the nitrification process as temperature affect nitrification. For example, Pálffy et al. (2017c) simulated in a passive CSO wetland  $\text{NH}_4\text{-N}$  adsorption in different seasons. They showed that in winter, 25% of the loaded nitrogen was nitrified over two dry days, while 60% was nitrified over 12 dry days. However, in this study, under the condition created in the 75/15 aeration strategy, after a short dry period of two days, the outlet concentrations remained stable due to a

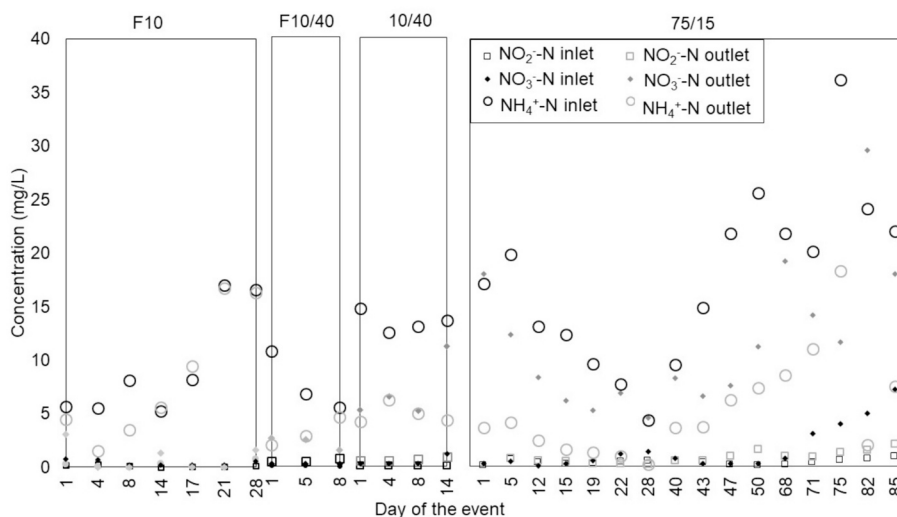
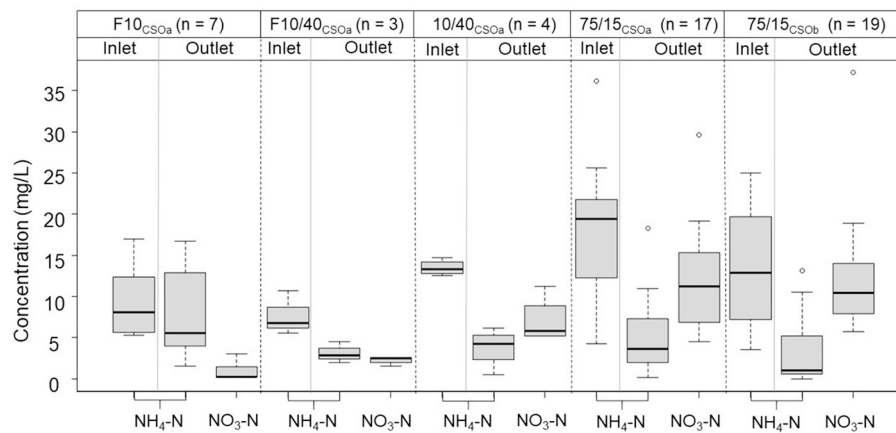


Fig. 5. Inlet and outlet concentrations of  $\text{NH}_4\text{-N}$ ,  $\text{NO}_3\text{-N}$  and  $\text{NO}_2\text{-N}$  for each tested aeration conditions in CSOa (F10, F10/40, 10/40 and 75/15).



**Fig. 6.** Tukey's boxplot of inlet and outlet concentrations of  $\text{NH}_4\text{-N}$  and outlet concentration of  $\text{NO}_3\text{-N}$  in the filters CSOa and CSOb. The number of tests performed (n) is indicated for each condition.

direct nitrification process that did not compromise the adsorption capacity of the media.

The median concentrations of  $\text{NH}_4\text{-N}$  and  $\text{NO}_3\text{-N}$  are shown in Fig. 6.

Conventional vertical CSO wetlands with passive aeration can achieve a high rate of nitrification. For example,  $\text{NH}_4\text{-N}$  removal in the range of 72% to 93% was reported by Pálffy et al. (2017a) and Ruppelt et al. (2018). However, the drawback of conventional vertical CSO wetlands is the requirement of a two-step process to achieve nitrification. The first step is ammonium adsorption during the feeding, and then during dry weather, when oxygen passes through the filter, nitrification occurs. Then, it is not always possible to guarantee either the amount of nitrified ammonium or the slow release of  $\text{NO}_3\text{-N}$  during the draining phase in this two-steps process (Tondera et al., 2018; Uhl and Dittmer, 2005).

Mechanical aeration may have induced nitrification zones in the filter, resulting in the transformation of  $\text{NH}_4\text{-N}$  to  $\text{NO}_3\text{-N}$  during the event. Much literature has reported consistent results regarding ammonium oxidation in TWs containing forced aeration (Boog et al., 2014; Dunqiu et al., 2012; John et al., 2020; Murphy et al., 2016), agreeing with the observed  $\text{NO}_3\text{-N}$  production in this study. However, the absence of anoxic zones makes the occurrence of denitrification less probable. In our study, total nitrogen within CSOa and CSOb was mostly removed through nitrogen assimilation into the biomass and direct nitrification, but denitrification did not occur due to a shortage of carbon source as outlet CODs is very low. Pálffy et al. (2017a) and Uhl and Dittmer (2005) noted in their CSO wetland similar results.

$\text{NH}_4\text{-N}$  and  $\text{NO}_3\text{-N}$  results of CSOa and CSOb were very similar. The  $\text{NH}_4\text{-N}$  removal rate reached up to 90%, and the median removal was 75% (CSOa) and 83% (CSOb) in the highly aerated condition (75/15). In terms of the  $\text{NH}_4\text{-N}$  removal, no significant differences were observed between CSOa and CSOb ( $p = 0.143$ ), despite the material surface area of sand potentially providing a higher adsorption capacity than gravel. Aeration may have favored direct nitrification during events, but it does not make adsorption a preponderant mechanism.

### 3.3. Redox potential

In the events in which redox potential was measured, there were consistent patterns related to aerobic and anoxic/anaerobic activity that were reproduced in more than one event. A general potential profile was observed at the outlet and inside the filter, 60 cm from the bottom. Whenever nitrification rates were high, redox potential generally was  $>300$  mV, indicating aerobic conditions. According to Murphy et al. (2016), redox potential  $>300$  mV hinders the process of denitrification, which is more effective under anaerobic conditions that promote facultative anaerobic denitrifying bacteria.

Fig. 7 shows measurements taken at 0.6 m from the bottom of the filter throughout the event, highlighting the contrast between the lowest and highest aeration conditions.

The response to aeration was immediate, and in conditions with higher aeration (75/15), the redox potential was never  $<300$  mV. Redox potential increased from  $-250$  mV to  $100$  mV within the 10 min aeration period (F10 aeration strategy). In addition, after the feeding, values went from  $130$  mV to negative values in 2 h once the aeration operation had ceased (Fig. 7). The redox measurements under aeration strategy F10 suggests that an anaerobic state predominated during the majority of the drainage period.

After feeding, each aeration strategy commonly exhibited a characteristic pattern in their redox potential curves at outlet of the filter. In aeration strategy F10, the redox curves were descended, while F10/40 and 10/40 showed plateaus before descending. Therefore, during F10/40 and 10/40, it was possible to achieve a steady state before oxygen depletion occurred. In aeration strategy 75/15, a transition point marked the curve's ascent and the redox potential of condition 75/15 ranged from  $350$  up to  $700$  mV at measurement points inside and outside of the filter. Measurements inside the filter (Fig. 7), showed the redox dropping from  $590$  to  $540$  mV, and from  $210$  to  $90$  mV with aeration strategies 75/15 and F10, respectively. Ruppelt et al. (2019) explained that the consumption of COD leads to a drop of the redox potential, with values around  $700$  mV being their maximum potential, as measured in aeration strategy 75/15. After the feeding period in the 75/15 aeration

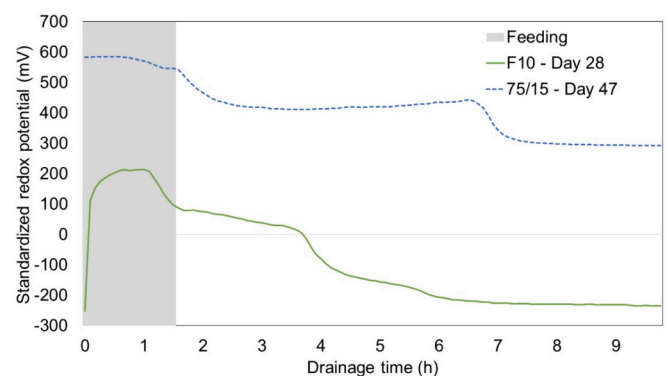


**Fig. 7.** Redox potential measured in two events in CSOa with a HL of 0.5 m. The first test under the aeration strategy F10 is indicated by the green line, and the second test under the 75/15 aeration strategy is indicated by the dashed blue line. Measurements were taken at 0.6 m depth from the bottom of the pilot. (For interpretation of the references to colour in this figure legend, the reader is referred to the web version of this article.)

strategy, the redox potential remained constant at approx. 300 mV during the drainage period.

### 3.4. Surface load and performances

After all trials, the cumulative hydraulic load onto filter CSOa reached  $40 \text{ m}^3 \cdot \text{m}^{-2}$  over 8 months and received  $>5 \text{ kg}_{\text{TSS}} \cdot \text{m}^{-2}$ . No hydraulic issues or signs of clogging were observed, as expected given gravel media. Other filters with similar media have operated without any signs of clogging for a longer time reaching  $10 \text{ kg}_{\text{TSS}} \cdot \text{m}^{-2} \cdot \text{y}^{-1}$  (Masi et al., 2023). The removal of solids was linearly correlated with solid loads independent of operational factors such as hydraulic loads or aeration conditions, whereas the organic loads removal were more dependent on the availability of oxygen in the pilot system. The result of aeration strategies F10/40 and 10/40 followed a pattern between loaded and removed COD mass, unlike F10, confirming that the oxygen supply is much lower than the oxygen demand. In the F10 aeration strategy, the correlation curve was shifted downward as the removal of CODs containing in CODt was inefficient and more dependent on other processes than aerobic oxidation.

Events under 75/15 aeration strategy in CSOa and CSOb showed strong correlations between the mass load applied and the load removed with close linearity curve. As observed in Fig. 8, events with an HL of 0.5 m tend to load a lower mass of COD and  $\text{NH}_4\text{-N}$ . Increasing the HL leads to higher organic loads, consistently following the same removal pattern. Additionally, increasing  $\text{NH}_4\text{-N}$  mass loads shows more dispersion in results of  $\text{NH}_4\text{-N}$  removal. However, a moderate correlation ( $R^2$ ) was still observed. Fig. 8 shows the correlation between the loaded and removed mass of COD and  $\text{NH}_4\text{-N}$ .

With aeration intervals of 75/15, a stable and linear relationship between applied and removed loads shows that performances stay stable for both COD and  $\text{NH}_4\text{-N}$  irrespective of the hydraulic and organic loads applied to the pilot systems during this study. Consequently, the dependence of the outlet concentration on the inlet concentration was greater. This appears logical as long as hydraulic retention time is stable throughout feeding and drainage phases and there is no lack of oxygen.

## 4. Conclusions

This study aimed to assess the impact of forced aeration on the performance and hydraulics of two pilot-scale CSO wetlands (CSOa and CSOb). Tests were conducted to compare the filter's hydrodynamics with and without aeration in two phases including the beginning of

feeding and ponding phase were conducted. Performance was evaluated under a range of aeration strategies and loading conditions. The optimal aeration strategy, as determined within CSOa, was reproduced within a second pilot scale system (CSOb) to gain insight into the impact on filter performance when designing it with a filtrating sand layer and gravel transient layer.

Tracer tests confirmed that in CSOa (without a sand layer), there are short-circuiting and reduced HRT at the beginning of an event when operating without aeration. It is evident that aeration has a significant impact on mixing and consequently HRT, ensuring a uniform flow distribution in both filters, particularly in CSOa. Once ponding conditions occur following loading, stopping the aeration will result in a more plug-flow condition.

Regarding pollutant removal, extended aeration intervals effectively degraded dissolved pollutants. Under the 75/15 aeration strategy, CSOa showed a median removal of 78% in CODs and 75% in  $\text{NH}_4\text{-N}$ , while CSOb exhibited removals of 83% in CODs and 92% in  $\text{NH}_4\text{-N}$ . The filters performed similarly, removal of TSS and COD were close to 95% and 85%, respectively, with a slight better removal efficiency in CSOb. The sand layer potentially trapped organic matter attached to solids, which improved TSS and COD removal in CSOb.

A well-balanced oxygen transfer to oxygen demand ratio was found to be a key factor in the aerobic degradation of dissolved COD and ammonia nitrification. In contrast to passive aeration filters, mechanical aeration maintained low concentrations of  $\text{NH}_4\text{-N}$  at the outlet due to the direct nitrification that occurs during the feeding and drainage phase. The system is not reliant on passive re-oxygenation after drainage to proceed with nitrification, which means that nitrate does not tend to accumulate and be washed out in subsequent events.

The correlation between mass loaded and removal rates remained consistent regardless of hydraulic loads. The filters demonstrated stability against varying surface loads, performing well for the most aerated aeration strategy (75/15).

The obtained results confirm the advantages of aerated vertical CSO wetlands treatment. Future work could contribute to understanding how long dry periods without loading might affect performances. Additionally, studies on the dynamics of nitrogen over time will contribute to understanding the influences of dry periods on nitrification rates and optimizing the aeration strategy and blower settings, thereby reducing energy costs.

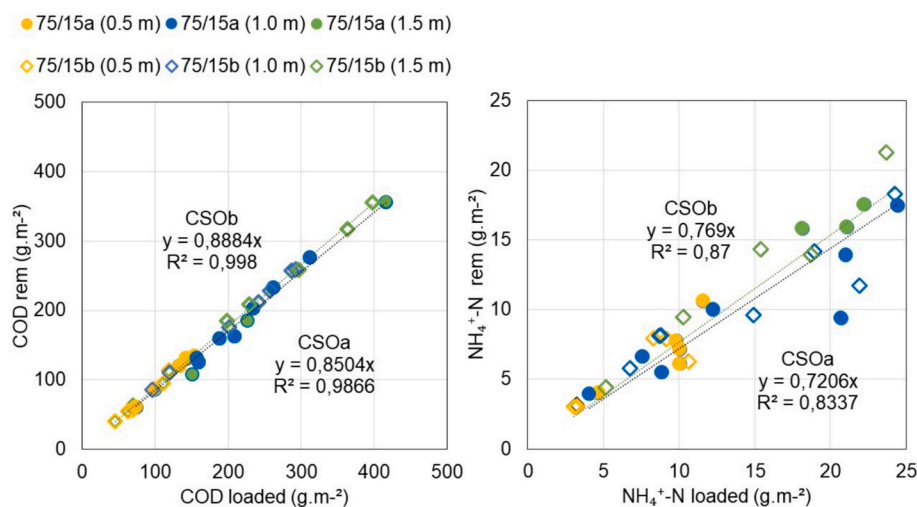


Fig. 8. Correlation of loaded and removed COD per event, on the left, and  $\text{NH}_4\text{-N}$ , on the right. Events in CSOa are indicated with an "a" and with a "b" for CSOb. The colors yellow, blue and green indicate different hydraulic loads. (For interpretation of the references to colour in this figure legend, the reader is referred to the web version of this article.)

## CRedit authorship contribution statement

**Daniella Portela:** Writing – review & editing, Writing – original draft, Visualization, Validation, Methodology, Investigation, Formal analysis, Data curation, Conceptualization. **Katharina Tondera:** Writing – review & editing, Writing – original draft, Validation, Supervision, Project administration, Methodology, Investigation, Conceptualization. **Stéphane Troesch:** Writing – review & editing, Writing – original draft, Resources, Project administration, Funding acquisition, Conceptualization. **Pascal Molle:** Writing – review & editing, Writing – original draft, Visualization, Validation, Supervision, Resources, Project administration, Methodology, Investigation, Funding acquisition, Formal analysis, Conceptualization.

## Declaration of competing interest

The authors declare that they have no known competing financial interests or personal relationships that could have appeared to influence the work reported in this paper.

## Data availability

Data will be made available on request.

## Acknowledgements

The authors would like to thank the financial support provided by the H2020 NICE project and extend appreciation to Olivier Garcia for the valuable technical support on the field.

## References

- Andrés-Doménech, I., Hernández-Crespo, C., Martín, M., Andrés-Valeri, V.C., 2018. Characterization of wash-off from urban impervious surfaces and SuDS design criteria for source control under semi-arid conditions. *Sci. Total Environ.* 612, 1320–1328. <https://doi.org/10.1016/j.scitotenv.2017.09.011>.
- ANR, 2013. *Système extensif pour la Gestion et le Traitement des Eaux Urbaines de temps de Pluie*. In: *Extensive Systems for the Management and Treatment of Urban Stormwaters*.
- Boog, J., Nivala, J., Aubron, T., Wallace, S., van Afferden, M., Müller, R.A., 2014. Hydraulic characterization and optimization of total nitrogen removal in an aerated vertical subsurface flow treatment wetland. *Bioresour. Technol.* 162, 166–174. <https://doi.org/10.1016/j.biortech.2014.03.100>.
- Boog, J., Nivala, J., Aubron, T., Mothes, S., van Afferden, M., Müller, R.A., 2018. Resilience of carbon and nitrogen removal due to aeration interruption in aerated treatment wetlands. *Sci. Total Environ.* 621, 960–969. <https://doi.org/10.1016/j.scitotenv.2017.10.131>.
- Collins, K.A., Lawrence, T.J., Stander, E.K., Jontos, R.J., Kaushal Newcomer, T.A., Grimm, N.B., Ekberg, M.L.C., 2010. Opportunities and challenges for managing nitrogen in urban stormwater: a review and synthesis. *Ecol. Eng.* 36, 1507–1519. <https://doi.org/10.1016/j.ecoleng.2010.03.015>.
- Cross, K., Tondera, K., Rizzo, A., Andrews, L., Pucher, B., Istenič, D., Karres, N., McDonald, R. (Eds.), 2021. *Nature-Based Solutions for Wastewater Treatment: A Series of Factsheets and Case Studies*. IWA Publishing. <https://doi.org/10.2166/9781789062267>.
- Dittmer, U., 2006. *Processes of Retention and Accumulation of Carbon and Nitrogen Compounds in Retention Soil Filters for Combined Sewer Overflow*. *Technischen Universität Kaiserslautern, Kaiserslautern*.
- Dotro, G., Langergraber, G., Molle, P., Nivala, J., Puigagut, J., Stein, O., von Sperling, M., 2017. *Biological Wastewater Treatment Series: Treatment Wetlands*. IWA.
- Dou, T., Troesch, S., Petitjean, A., Gábor, P.T., Esser, D., 2017. Wastewater and Rainwater Management in Urban Areas: a Role for Constructed Wetlands. *Procedia Environ. Sci.* 37, 535–541. <https://doi.org/10.1016/j.proenv.2017.03.036>.
- Dunqiu, W., Shaoyuan, B., Mingyu, W., Qinglin, X., Yinian, Z., Hua, Z., 2012. Effect of Artificial Aeration, Temperature, and Structure on Nutrient Removal in Constructed floating Islands. *Water Environ. Res.* 84, 405–410. <https://doi.org/10.2175/106143012X1334768384684>.
- DWA-A178, 2019. *Retentionsbodenfilteranlagen. Retention Soil Filter Sites*. German Association for Water, Wastewater and Waste. Hennef.
- Fournel, J., 2012. *Systemes Extensifs De Gestion Et De Traitement Des Eaux Urbaines De Temps De Pluie*. Université Montpellier II, France.
- Gasperi, J., Zgheib, S., Cladière, M., Rocher, V., Moilleron, R., Chebbo, G., 2012. Priority pollutants in urban stormwater: part 2 – Case of combined sewers. *Water Res.* 46, 6693–6703. <https://doi.org/10.1016/j.watres.2011.09.041>.
- Gioia, A., Lioi, B., Totaro, V., Molfetta, M.G., Apollonio, C., Bisantino, T., Iacobellis, V., 2021. Estimation of Peak Discharges under Different Rainfall
- Depth–Duration–Frequency Formulations. *Hydrology* 8, 150. <https://doi.org/10.3390/hydrology8040150>.
- Headley, T.R., Kadlec, R.H., 2007. Conducting hydraulic tracer studies of constructed wetlands: a practical guide. *Ecology & Hydrobiology* 7, 269–282. [https://doi.org/10.1016/S1642-3593\(07\)70110-6](https://doi.org/10.1016/S1642-3593(07)70110-6).
- Headley, T., Nivala, J., Kassa, K., Olsson, L., Wallace, S., Brix, H., van Afferden, M., Müller, R., 2013. *Escherichia coli* removal and internal dynamics in subsurface flow ecotechnologies: Effects of design and plants. *Ecol. Eng.* 61, 564–574. <https://doi.org/10.1016/j.ecoleng.2013.07.062>.
- IPCC, 2023. In: Team, Core Writing, Lee, H., Romero, J. (Eds.), *Climate Change 2023: Synthesis Report. Contribution of Working Groups I, II and III to the Sixth Assessment Report of the Intergovernmental Panel on Climate Change*. IPCC, Geneva, Switzerland. <https://doi.org/10.59327/IPCC/AR6-9789291691647>.
- Intergovernmental Panel on Climate Change (IPCC).
- John, Y., Langergraber, G., Adyel, T.M., Emery David, V., 2020. Aeration intensity simulation in a saturated vertical up-flow constructed wetland. *Sci. Total Environ.* 708, 134793. <https://doi.org/10.1016/j.scitotenv.2019.134793>.
- Kadlec, R., Wallace, S., 2008. *Treatment Wetlands*, 2nd ed. Taylor & Francis Group.
- Madoux-Humery, A.-S., Dorner, S.M., Sauvé, S., Aboufadel, K., Galarneau, M., Servais, P., Prévost, M., 2015. Temporal analysis of E. Coli, TSS and wastewater micropollutant loads from combined sewer overflows: implications for management. *Environ. Sci.: Processes Impacts* 17, 965–974. <https://doi.org/10.1039/C5EM00093A>.
- Masi, F., Rizzo, A., Bresciani, R., Conte, G., 2017. Constructed wetlands for combined sewer overflow treatment: Ecosystem services at Gorla Maggiore, Italy. *Ecol. Eng.* 98, 427–438. <https://doi.org/10.1016/j.ecoleng.2016.03.043>.
- Masi, F., Sarti, C., Cincinelli, A., Bresciani, R., Martinuzzi, N., Bernasconi, M., Rizzo, A., 2023. Constructed wetlands for the treatment of combined sewer overflow upstream of centralized wastewater treatment plants. *Ecol. Eng.* 193. <https://doi.org/10.1016/j.ecoleng.2023.107008>.
- Meyer, D., Molle, P., Esser, D., Troesch, S., Dittmer, U., Masi, F., 2013. Constructed wetlands for combined sewer overflow treatment—comparison of German, French and Italian approaches. *Water* 5, 12. <https://doi.org/10.3390/w5010001>.
- Miyazaki, C.K., Morvannou, A., Higelin, E., Nivala, J., Molle, P., 2023. Aeration strategies and total nitrogen removal in a hybrid aerated treatment wetland. *Blue-Green Systems* 5, 321–335. <https://doi.org/10.2166/bgs.2023.045>.
- Murphy, C., Rajabzadeh, A.R., Weber, K.P., Nivala, J., Wallace, S.D., Cooper, D.J., 2016. Nitrification cessation and recovery in an aerated saturated vertical subsurface flow treatment wetland: Field studies and microscale biofilm modeling. *Bioresour. Technol.* 209, 125–132. <https://doi.org/10.1016/j.biortech.2016.02.065>.
- Nivala, J., Kahl, S., Boog, J., Van Afferden, M., Reemtsma, T., Müller, R.A., 2019. Dynamics of emerging organic contaminant removal in conventional and intensified subsurface flow treatment wetlands. *Sci. Total Environ.* 649, 1144–1156. <https://doi.org/10.1016/j.scitotenv.2018.08.339>.
- Oral, H.V., Carvalho, P., Gajewska, M., Ursino, N., Masi, F., Hullebusch, E.D., Kazak, J.K., Exposito, A., Cipolletta, G., Andersen, T.R., Finger, D.C., Simperler, L., Regelsberger, M., Rous, V., Radinja, M., Buttiglieri, G., Krzeminski, P., Rizzo, A., Dehghanian, K., Nikolova, M., Zimmermann, M., 2020. A review of nature-based solutions for urban water management in European circular cities: a critical assessment based on case studies and literature. *Blue-Green Systems* 2, 112–136. <https://doi.org/10.2166/bgs.2020.932>.
- Pálffy, T.G., Gerodolle, M., Gourdon, R., Meyer, D., Troesch, S., Molle, P., 2017a. Performance assessment of a vertical flow constructed wetland treating unsettled combined sewer overflow. *Water Sci. Technol.* 75, 2586–2597. <https://doi.org/10.2166/wst.2017.126>.
- Pálffy, T.G., Gourdon, R., Meyer, D., Troesch, S., Molle, P., 2017b. Model-based optimization of constructed wetlands treating combined sewer overflow. *Ecol. Eng.* 101, 261–267. <https://doi.org/10.1016/j.ecoleng.2017.01.020>.
- Pálffy, T.G., Gourdon, R., Meyer, D., Troesch, S., Olivier, L., Molle, P., 2017c. Filling hydraulics and nitrogen dynamics in constructed wetlands treating combined sewer overflows. *Ecol. Eng.* 101, 137–144. <https://doi.org/10.1016/j.ecoleng.2017.01.008>.
- Phillips, P.J., Chalmers, A.T., Gray, J.L., Kolpin, D.W., Foreman, W.T., Wall, G.R., 2012. Combined Sewer Overflows: an Environmental source of Hormones and Wastewater Micropollutants. *Environ. Sci. Technol.* 46, 5336–5343. <https://doi.org/10.1021/es3001294>.
- Rizzo, A., Tondera, K., Pálffy, T.G., Dittmer, U., Meyer, D., Schreiber, C., Zacharias, N., Ruppelt, J.P., Esser, D., Molle, P., Troesch, S., Masi, F., 2020. Constructed wetlands for combined sewer overflow treatment: a state-of-the-art review. *Sci. Total Environ.* 727, 138618. <https://doi.org/10.1016/j.scitotenv.2020.138618>.
- Ruppelt, J.P., Tondera, K., Schreiber, C., Kistemann, T., Pinnekamp, J., 2018. Reduction of bacteria and somatic coliphages in constructed wetlands for the treatment of combined sewer overflow (retention soil filters). *Int. J. Hyg. Environ. Health* 221, 727–733. <https://doi.org/10.1016/j.ijheh.2018.04.011>.
- Ruppelt, J.P., Tondera, K., Vorenhout, M., Van der Weken, L., Pinnekamp, J., 2019. Redox potential as a method to evaluate the performance of retention soil filters treating combined sewer overflows. *Sci. Total Environ.* 650, 1628–1639. <https://doi.org/10.1016/j.scitotenv.2018.09.043>.
- Salerno, F., Gaetano, V., Gianni, T., 2018. Urbanization and climate change impacts on surface water quality: Enhancing the resilience by reducing impervious surfaces. *Water Res.* 144, 491–502. <https://doi.org/10.1016/j.watres.2018.07.058>.
- Schmitt, N., Wanko, A., Laurent, J., Bois, P., Molle, P., Mosé, R., 2015. Constructed wetlands treating stormwater from separate sewer networks in a residential Strasbourg urban catchment area: Micropollutant removal and fate. *J. Environ. Chem. Eng.* 3, 2816–2824. <https://doi.org/10.1016/j.jece.2015.10.008>.

- Seidl, M., Servais, P., Mouchel, J.M., 1998. Organic matter transport and degradation in the river Seine (France) after a combined sewer overflow. *Water Res.* 32, 3569–3580. [https://doi.org/10.1016/S0043-1354\(98\)00169-9](https://doi.org/10.1016/S0043-1354(98)00169-9).
- Séranne, L., Prost-Boucle, S., Clément, R., Nivala, J., Gillot, S., Molle, P., 2021. Influence of Airflow, Material Type, and Dripline Density on Gas Transfer and Bubble Pathways in Aerated Vertical Flow Treatment Wetlands. University of Natural Resources and Life Sciences, Vienna.
- Stefanakis, A., 2019. The Role of Constructed Wetlands as Green Infrastructure for Sustainable Urban Water Management. *Sustainability* 11, 6981. <https://doi.org/10.3390/su11246981>.
- Tchobanoglous, G., Burton, F.L., Stensel, H.D., Metcalf & Eddy, Inc (Eds.), 2003. *Wastewater Engineering: Treatment and Reuse*, 4. Ed., Internat. Ed., [Nachdr.]. Ed. McGraw-Hill Series in Civil and Environmental Engineering. McGraw-Hill, Boston, Mass.
- Tondera, K., 2019. Evaluating the performance of constructed wetlands for the treatment of combined sewer overflows. *Ecol. Eng.* 137, 53–59. <https://doi.org/10.1016/j.ecoleng.2017.10.009>.
- Tondera, K., Koenen, S., Pinnekamp, J., 2013. Survey monitoring results on the reduction of micropollutants, bacteria, bacteriophages and TSS in retention soil filters. *Water Sci. Technol.* 68, 1004–1012. <https://doi.org/10.2166/wst.2013.340>.
- Tondera, K., Blecken, G.-T., Chazarenc, F., Tanner, C.C. (Eds.), 2018. *Ecotechnologies for the Treatment of Variable Stormwater and Wastewater Flows*, SpringerBriefs in Water Science and Technology. Springer International Publishing, Cham. <https://doi.org/10.1007/978-3-319-70013-7>.
- Tondera, K., Rizzo, A., Molle, P., 2021. Treatment wetlands for combined sewer overflow. In: *Nature-Based Solutions for Wastewater Treatment*. IWA Publishing, p. 344.
- Uhl, M., Dittmer, U., 2005. Constructed wetlands for CSO treatment: an overview of practice and research in Germany. *Water Sci. Technol.* 51, 23–30.
- Vymazal, J., 1999. Removal of BOD5 in constructed wetlands with horizontal sub-surface flow: Czech experience. *War. Sci. Tech* 40, 133–138. [https://doi.org/10.1016/S0273-1223\(99\)00456-4](https://doi.org/10.1016/S0273-1223(99)00456-4).